



Strathprints Institutional Repository

Su, Dongxu and Zheng, Rencheng and Nakano, Kimihiko and Cartmell, Matthew P (2016) Stabilisation of the high energy orbit for a nonlinear energy harvester with variable damping. Proceedings of the Institution of Mechanical Engineers, Part C: Journal of Mechanical Engineering Science, 230 (12). pp. 2003-2012. ISSN 0954-4062 , <http://dx.doi.org/10.1177/0954406215590169>

This version is available at <http://strathprints.strath.ac.uk/57178/>

Strathprints is designed to allow users to access the research output of the University of Strathclyde. Unless otherwise explicitly stated on the manuscript, Copyright © and Moral Rights for the papers on this site are retained by the individual authors and/or other copyright owners. Please check the manuscript for details of any other licences that may have been applied. You may not engage in further distribution of the material for any profitmaking activities or any commercial gain. You may freely distribute both the url (<http://strathprints.strath.ac.uk/>) and the content of this paper for research or private study, educational, or not-for-profit purposes without prior permission or charge.

Any correspondence concerning this service should be sent to Strathprints administrator: strathprints@strath.ac.uk



Stabilisation of the high-energy orbit for a non-linear energy harvester with variable damping

Proc IMechE Part C:
J Mechanical Engineering Science
0(0) 1–10
© IMechE 2015
Reprints and permissions:
sagepub.co.uk/journalsPermissions.nav
DOI: 10.1177/0954406215590169
pic.sagepub.com
SAGE

Dongxu Su¹, Rencheng Zheng², Kimihiko Nakano³ and Matthew P Cartmell⁴

Abstract

The non-linearity of a hardening-type oscillator provides a wider bandwidth and a higher energy harvesting capability under harmonic excitations. Also, both low- and high-energy responses can coexist for the same parameter combinations at relatively high excitation levels. However, if the oscillator's response happens to coincide with the low-energy orbit then the improved performance achieved by the non-linear oscillator over that of its linear counterpart, could be impaired. This is therefore the main motivation for stabilisation of the high-energy orbit. In the present work, a schematic harvester design is considered consisting of a mass supported by two linear springs connected in series, each with a parallel damper, and a third-order non-linear spring. The equivalent linear stiffness and damping coefficients of the oscillator are derived through variation of the damper element. From this adjustment the variation of the equivalent stiffness generates a corresponding shift in the frequency–amplitude response curve, and this triggers a jump from the low-energy orbit to stabilise the high-energy orbit. This approach has been seen to require little additional energy supply for the adjustment and stabilisation, compared with that needed for direct stiffness tuning by mechanical means. Overall energy saving is of particular importance for energy harvesting applications. Subsequent results from simulation and experimentation confirm that the proposed method can be used to trigger a jump to the desirable state, thereby introducing a beneficial addition to the performance of the non-linear hardening-type energy harvester that improves overall efficiency and broadens the bandwidth.

Keywords

Energy harvesting, hardening-type Duffing oscillator, tunable stiffness, damping variation

Date received: 20 October 2014; accepted: 6 May 2015

Introduction

Efficient energy harvesting from ambient environmental vibration is of great current interest as a means of providing a free power supply for small-scale electronics. Compared with other energy sources, vibrations are generally ubiquitous^{1,2} and one can readily envisage autonomous wireless sensor nodes and microsystems being usefully powered by such vibration, particularly in inaccessible or hostile environments. This paper presents a comprehensive analytical and experimental study of the benefits of stabilisation of the high-energy orbit in a novel hardening-type non-linear energy harvester in order to improve the efficiency of energy harvesting.

One important feature of conventional vibration-driven energy harvesters is that they provide maximum power when the resonant frequency of the device matches the environmental excitation frequency.^{3–7} However, because of the significantly reduced performance under off-resonance conditions,

and the difficulty in directly matching the linear resonance of most practical mechanical devices to the variable frequencies present in an environmental ambient vibration source, research effort has been put into eliminating such shortcomings in linear devices. For instance, a mechanical bandwidth filter comprising piezoelectric cantilevers of various lengths, and with tip masses attached to a common base, has been considered by Shahruz^{8,9} as a solution for increasing the bandwidth of response. Rastegar

¹Graduate School of Engineering, The University of Tokyo, Tokyo, Japan

²Institute of Industrial Science, The University of Tokyo, Tokyo, Japan

³Interfaculty Initiative in Information Studies, The University of Tokyo, Japan

⁴Department of Mechanical Engineering, University of Sheffield, Sheffield, UK

Corresponding author:

Dongxu Su, Graduate School of Engineering, The University of Tokyo, 4-6-1 Komaba Meguro-ku, Tokyo 153-8505, Japan.
Email: sudx@iis.u-tokyo.ac.jp

et al.¹⁰ designed an ingenious frequency up-conversion mechanism as a concept for two-stage energy harvesting. The low-frequency vibration of the primary vibrating unit (i.e. the mass) can be transferred to high-frequency vibrations of the secondary vibration units (i.e. the piezoelectric cantilevers), hence providing a single-frequency robust vibration energy harvesting solution in low-frequency excitation scenarios.

Subsequently, the exploitation of non-linear phenomenology started to take over with variations of the Duffing oscillator providing several interesting possibilities.^{11–16} A hardening-type oscillator was investigated by Mann et al.¹⁷ and it was found that at relatively high sinusoidal excitation levels, both low and high-energy responses can coexist for the same parameter combinations. When compared with a linear oscillator using similar parameters the effectiveness of a non-linear energy harvesting device can apparently be increased over certain frequency ranges when operating on the high-energy orbit. In addition to this technique a monostable non-linear device using the piezoelectric effect was proposed by Stanton et al.¹⁸ The response of this system showed an increase in bandwidth and the resulting experimental results verified a distinct capability for outperforming the linear approach.

In the studies just described slow forward or backward sweeps of the excitation frequency are required as a precondition in order to stabilise the high-energy orbit, despite the implementation challenge that this offers in practice, and in fact this is a formidable requirement for satisfying ideal harvesting conditions. In order to solve this problem a load circuit with a switch between the conventional load, a negative resistance circuit, and a switching control law dependent on the amplitude of the oscillator's response, were introduced and the effects of such a sub-system studied numerically by Masuda et al.¹⁹ The effect of this was to impart a capability for self-excitation in order to entrain the oscillator with the excitation exclusively onto the high-energy orbit. However, besides the additional electrical energy required to drive the circuit, switching this approach also consumes part of the harvested energy in order to destabilise the low-energy orbit and trigger the jump. Although the technique works well enough it is not ideal in the context of energy harvester self sustainability and overall efficiency.

Another solution to this problem is to vary the stiffness of the energy harvester. Su et al.²⁰ have successfully shown in an experiment that it is possible to tune both of linear and non-linear stiffnesses of a hardening-type energy harvester in order to trigger a jump to the high-energy orbit, and to achieve this by adjusting the distance between magnets used in the proposed design. A linear DC motor and a lead screw were utilised in that work to tune the stiffness and the energy consumed for this form of mechanical tuning was the main shortcoming that was found. A similar effort to tune the stiffness of a linear vibration-based generator was

reported by Zhu et al.²¹ Inspired by a linear vibration isolation system with variable stiffness as proposed by Lin et al.,²² the method of damping variation is used in this paper to change the equivalent linear stiffness of a non-linear harvester for stabilising the high-energy orbit. It provides an advantage for practical implementation because of the fact that it consumes much less energy to vary the damping compared with directly tuning the stiffness using the mechanical method, especially when an electromagnetic damper is adopted. It should be noted that this kind of electrical damper was successfully used for a self powered vehicle suspension by Nakano et al.,²³ where the electrical damping was tuned by varying the load resistance in the electrical drive circuit. A novel non-linear vibrational energy harvester is designed in this paper whose equivalent linear stiffness can be changed by just varying the damping. Moreover, the proposed principle of stabilising the high-energy orbit is demonstrated by analysis of the variation in the frequency–amplitude response curves during the tuning process thereby validating different damping coefficient tuning methods.

The work reported in this paper is organised as follows. The next section describes the mathematical model of a stiffness tunable device, and the expressions for equivalent stiffness and damping coefficient are derived. This is followed by a frequency–response analysis of the system under harmonic base excitation. The corresponding influence on the frequency response during the process of stiffness tuning is then investigated. Finally, the effectiveness of the theory is confirmed by a series of simulation and experimental results.

Methodology

Apparatus illustrations and modelling of the energy harvester

A schematic diagram for an energy harvester is shown in Figure 1. It is composed of two linear springs connected in series, with two dampers in parallel with the springs, and a third order non-linear spring. It should be noted that the model is a one-degree-of-freedom system because the linear springs are connected at a node which is an effectively massless point. The equivalent linear stiffness of the system can be tuned by adjusting the damping coefficient of controllable damper c_2 .

The governing equations for the motion of the system shown can be stated as

$$m\ddot{x} = -k_2(x - x_p) - c_2(\dot{x} - \dot{x}_p) - k_3x^3 + F \quad (1a)$$

$$k_1x_p + c_1\dot{x}_p = k_2(x - x_p) + c_2(\dot{x} - \dot{x}_p) \quad (1b)$$

where m is the mass, k_1, k_2 are the stiffness coefficients of the springs, and c_1, c_2 are the damping shown in Figure 1. x and x_p are the displacements of the mass

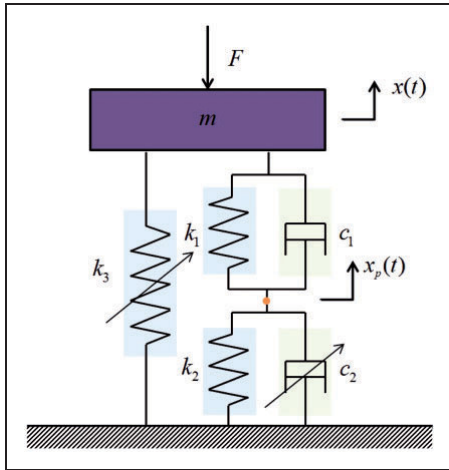


Figure 1. Schematic diagram of the stiffness, tunable, hardening-type energy harvester.

and the connection point of the springs, respectively. The single-frequency harmonic excitation is given by $F = f \cos \omega t$.

The harmonic balance method is applied to generate the responses. The harvester response is presumed to be accurately modelled by a truncated Fourier series, where the number of terms dictates the accuracy of the intended solution.²³ This type of motion maintains a dominant fundamental frequency at the frequency of excitation. Hence, equations (2a) and (2b) can represent the assumed Fourier series expansion of the displacements of the mass, and connection point, respectively

$$x = a_1 \sin \omega t + b_1 \cos \omega t \quad (2a)$$

$$x_p = a_2 \sin \omega t + b_2 \cos \omega t \quad (2b)$$

where $X^2 = a_1^2 + b_1^2$ and $X_p^2 = a_2^2 + b_2^2$. X and X_p therefore represent the corresponding displacement amplitudes. Equations (2a) and (2b), and the time derivatives, are substituted into equations (1a) and (1b). Ignoring higher order harmonics and equating the coefficients of the harmonic terms $\cos \omega t$ and $\sin \omega t$, four equations are obtained from the mechanical equation as follows

$$k_1 a_2 - c_1 b_2 \omega = k_2 (a_1 - a_2) - c_2 (b_1 - b_2) \omega \quad (3a)$$

$$k_1 b_2 - c_1 a_2 \omega = k_2 (b_1 - b_2) - c_2 (a_1 - a_2) \omega \quad (3b)$$

$$-ma_1 \omega^2 + k_2 (a_1 - a_2) - c_2 (b_1 - b_2) \omega + \frac{3}{4} k_3 (b_1^2 a_1 + a_1^3) = 0 \quad (3c)$$

$$-mb_1 \omega^2 + k_2 (b_1 - b_2) + c_2 (a_1 - a_2) \omega + \frac{3}{4} k_3 (a_1^2 b_1 + b_1^3) = f \quad (3d)$$

Equations (3a) and (3b) are solved in terms of a_2 and b_2 , then substituted into equations (3c) and (3d). The latter are squared and summed to produce the following equation as

$$\begin{aligned} & \frac{9}{16} k_3^2 X^6 + \frac{3}{2} k_3 \left[\frac{k_1^2 k_2 + k_2^2 k_1 + (c_1^2 k_2 + c_2^2 k_1) \omega^2}{(k_1 + k_2)^2 + (c_1 + c_2)^2 \omega^2} - m \omega^2 \right] X^4 \\ & + \left\{ \frac{k_1^2 k_2 + k_2^2 k_1 + (c_1^2 k_2 + c_2^2 k_1) \omega^2}{(k_1 + k_2)^2 + (c_1 + c_2)^2 \omega^2} - m \omega^2 \right. \\ & \left. + \left[\frac{k_1^2 c_2 + k_2^2 c_1 + (c_2^2 c_1 + c_1^2 c_2) \omega^3}{(k_1 + k_2)^2 + (c_1 + c_2)^2 \omega^2} \right]^2 \right\} X^2 = f^2 \end{aligned} \quad (4)$$

For the equivalent model of the system, the corresponding relationship between the frequency and amplitude of the response can be given as²⁴

$$\begin{aligned} & \frac{9}{16} k_3^2 X^6 + \frac{3}{2} k_3 (k_e - m \omega^2) X^4 \\ & + \left[(k_e - m \omega^2)^2 + c_e^2 \omega^2 \right] X^2 = f^2 \end{aligned} \quad (5)$$

where k_e is the equivalent linear stiffness coefficient, and c_e is the equivalent damping coefficient. From equations (4) and (5), the equivalent stiffness and damping coefficients can be expressed as

$$k_e = \frac{k_1 k_2 (k_1 + k_2) + (c_1^2 k_2 + c_2^2 k_1) \omega^2}{(k_1 + k_2)^2 + (c_1 + c_2)^2 \omega^2} \quad (6)$$

$$c_e = \frac{k_1^2 c_2 + k_2^2 c_1 + c_1 c_2 (c_1 + c_2) \omega^2}{(k_1 + k_2)^2 + (c_1 + c_2)^2 \omega^2} \quad (7)$$

A set of physically reasonable parameters used for simulation is shown in Table 1. These data are also used for the numerical examples afterwards.

The equivalent stiffness and damping coefficients as functions of c_2 and the stiffness coefficient ratio k_2/k_1 are plotted in Figures 2 and 3, respectively. It is noted that the equivalent stiffness increases with increasing c_2 and that it can be tuned within a larger range when k_2/k_1 is smaller, as shown in Figure 2. However, from Figure 3, it can be shown that the equivalent damping increases first, then decrease with increasing c_2 , and that smaller k_2/k_1 can cause a greater equivalent damping when a certain value of the damping coefficient c_2 is applied.

The effects of damping coefficient variation on the response

The tuning of the damping coefficient can cause a change in the equivalent stiffness, and then a further influence on the frequency–amplitude response curve of the oscillator. The detailed principle of the proposed method is presented in this section. Figure 4

Table 1. Parameters of the vibrational energy harvester.

| Parameter | m | c_1 | k_1 | α | F | ω |
|-----------|------|---------|---------|---------------------------------|-----|----------|
| Value | 1 kg | 1.2Nm/s | 1000N/m | $2.45 \times 10^6 \text{N/m}^3$ | 1 N | 5.2 Hz |

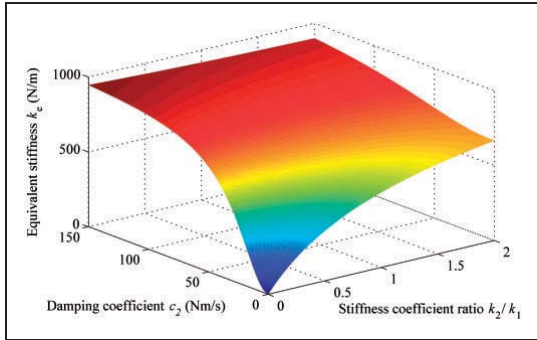


Figure 2. Equivalent stiffness coefficient as a function of c_2 and stiffness coefficient ratio k_2/k_1 .

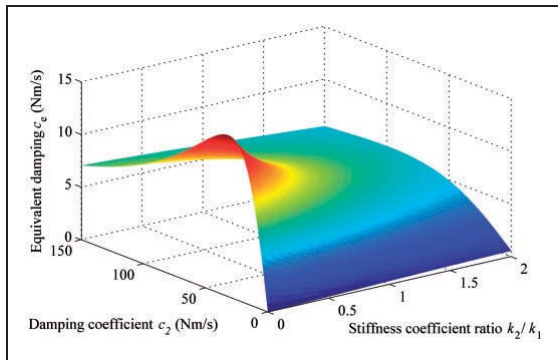


Figure 3. Equivalent damping coefficient as a function of c_2 and stiffness coefficient ratio k_2/k_1 .

shows the frequency–response curves under different values of damping coefficient c_2 according to equation (4), while the other parameters shown in Table 1 are kept constant. Variations in the damping coefficient have an influence on both the jump-up and jump-down frequencies. By increasing the linear stiffness, the frequency–response curve shows a movement to the right.

The process of triggering the jump is also illustrated in Figure 4. It is assumed that the energy harvester is oscillating at point A when c_2 is equal to 5 Ns/m, with this point located in the low-energy orbit, and then by starting to increase c_2 , the shape of the frequency–response curve slowly varies, as shown in Figure 4. The operating point jumps to point B when the frequency of the excitation exceeds the jump-up frequency. The oscillator is now operating in the preferred orbit. However, variation in the stiffness also decreases the amplitude of the response. Thus, following the high-energy orbit, the operating

point subsequently moves to C by decreasing the damping coefficient c_2 . It is noted that in the process of tuning the damping coefficient there is a possibility that the multi-valued frequency–response curve disappears (for $c_2 = 20$ Ns/m) because the equivalent damping coefficient initially increases with c_2 , as shown in Figure 3. This phenomenon does not influence the jump from point A to B, but the movement from point B to C and this is further discussed below.

The jump-up and jump-down frequencies of a hardening-type, lightly damped Duffing oscillator with linear viscous damping can be found in the literature. Brennan et al.²⁴ presented a full set of expressions for the analytical solution using the harmonic balance method, and made some comparisons with other expressions. To analyse the tuning process quantitatively, and for the sake of clarity, the approach taken by Brennan is followed.

The non-dimensional form of equation (5) can be expressed as

$$\frac{9}{16}\beta^2 U^6 + \frac{3}{2}\beta(1 - \Omega^2)U^4 + \left((1 - \Omega^2)^2 + (2\zeta\Omega)^2 \right) U^2 = 1 \quad (8)$$

where $\Omega = \frac{\omega}{\omega_n}$, $\omega_n = \sqrt{\frac{k_e}{m}}$, $U = \frac{k_e X}{F}$, $\beta = \frac{k_3 f^2}{k_e^3}$ and $\zeta = \frac{c_e}{2m\omega_n}$.

To find the analytic expressions for the jump-up and jump down frequencies, equation (8) is rearranged as

$$U^2 \Omega^4 + \left((4\zeta^2 - 2)U^2 - \frac{3}{2}\beta U^4 \right) \Omega^2 + \left(U + \frac{3}{4}\beta U^3 \right)^2 = 1 \quad (9)$$

Solving equation (8) and assuming that $\zeta^2 \ll 1$, the positive solutions are

$$\Omega_{1,2} \approx \sqrt{\frac{3\beta U^2}{4} + 1} \pm \frac{\sqrt{1 - 4\zeta^2 U^2 - 3\beta \zeta^2 U^4}}{U} \quad (10)$$

It should be noted that when the jump-up phenomenon occurs, this frequency is weakly dependent upon the damping ratio. Thus, by setting $\zeta = 0$ and finding the point at $\frac{d\Omega_{1,2}}{dU} = 0$, the non-dimensional displacement amplitude of the jump-up frequency can be given as

$$U_u \approx \left(\frac{2}{3\beta} \right)^{1/3} \quad (11)$$

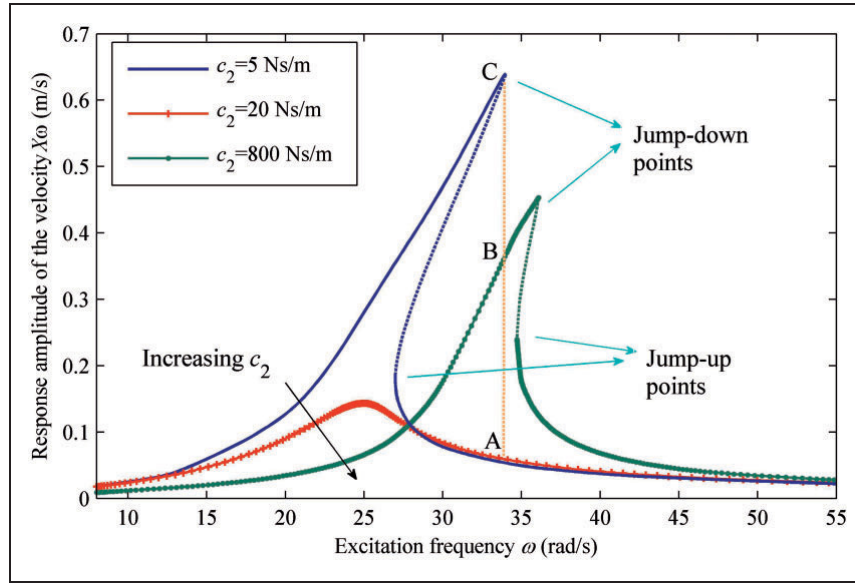


Figure 4. Frequency–response curve of a hardening-type system.

Substituting equation (11) into equation (10) gives the jump-up frequency

$$\Omega_u \approx \sqrt{1 + \frac{3}{2} \left(\frac{3\beta}{2} \right)^{1/3}} \quad (12)$$

To trigger a jump to the high-energy orbit, the dimensional jump frequency ω_u should be higher than the excitation frequency ω . Hence, from equation (12), the minimum equivalent stiffness coefficient for triggering a jump is defined by

$$k'_e = m\omega^2 - \left(\frac{3}{2} \right)^{4/3} (\alpha F^2)^{1/3} \quad (13)$$

It is assumed that the electrical damping is small and $c_1 \ll c_2$. By setting $c_1 = 0$, the corresponding minimum control damping coefficient can be given by equation (6) as

$$c_{2u} = \sqrt{\frac{k'_e(k_1 + k_2)^2 - k_1 k_2 (k_1 + k_2)}{\omega^2 (k_1 - k'_e)}} \quad (14)$$

Using equation (14), and substituting equation (13) into equation (7), the required equivalent damping coefficient to get the target equivalent stiffness can be expressed as

$$c_{eu} = \frac{\sqrt{(k'_e(k_1 + k_2)^2 - k_1 k_2 (k_1 + k_2))(k_1 - k'_e)}}{\omega(k_1 + k_2)} \quad (15)$$

To increase the jump-up frequency tuning range as much as possible, it is necessary to analyse the influence of the parameters k_2/k_1 and αF^2 on the ratio between the maximum and minimum jump-up frequencies and this can be expressed as the following frequency ratio

$$\frac{\omega_{u \max}}{\omega_{u \min}} = \frac{\sqrt{k_{\max} + (3/2)^{4/3} (\alpha F^2)^{1/3}}}{\sqrt{k_{\min} + (3/2)^{4/3} (\alpha F^2)^{1/3}}} \quad (16)$$

where $k_{\max} = k_1$ when $c_1 = c_2 = 0$ and $k_{\min} = k_1 k_2 / (k_1 + k_2)$ when $c_2 \rightarrow \infty$.

Assuming that $k_1 = 1000 \text{ N/m}$, the jump-up frequency ratio as a function of k_2/k_1 and αF^2 is shown in Figure 5, where αF^2 governs the degree of non-linearity and the excitation amplitude.

It is noted that a smaller stiffness coefficient ratio k_2/k_1 is propitious for increasing the tuning range. Additionally, the weaker non-linearity and smaller excitation amplitude can achieve a similar effect for increasing the jump-up frequency tuning range.

As analysed above, it is possible to trigger a jump to the high-energy orbit by tuning the damping until the jump-up frequency exceeds the frequency of the excitation. However, under some conditions it is necessary to continue to decrease the equivalent stiffness to close to the jump-down frequency, which is the peak response point of the oscillator. It should be noted that the equivalent damping of the system also varies besides the equivalent stiffness in the process of damping variation, as shown in Figure 3, which has strong influence on the occurrence of the multi-valued frequency–amplitude curve and the value of the jump-down frequency. Thus, excessive

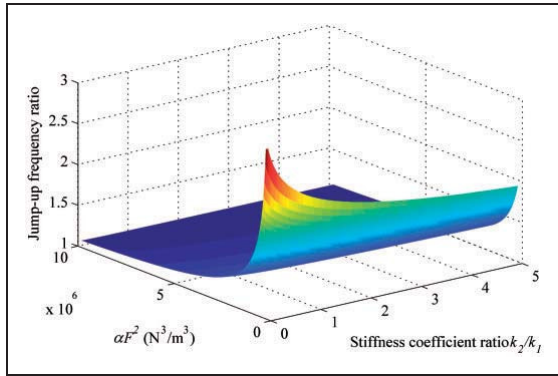


Figure 5. Jump-up frequency ratio as a function of k_2/k_1 and αF^2 .

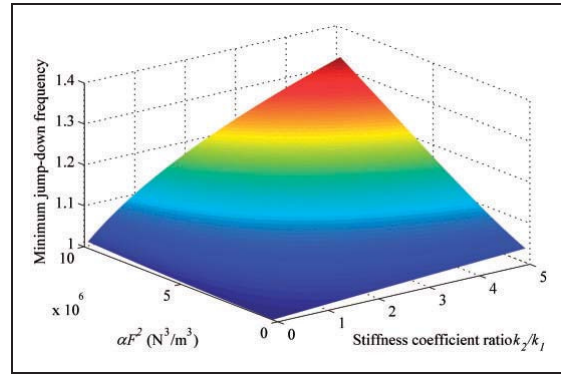


Figure 6. Minimum jump-down frequency as a function of k_2/k_1 and αF^2 .

equivalent damping during the tuning process (point B to point C shown in Figure 4) may again lead to an undesirable jump-down to the low-energy orbit.

The condition for the multi-valued frequency–amplitude curve to occur is defined as²⁴

$$\beta \geq \frac{2^8}{3^{5/2}} \zeta^3 \quad (17)$$

Equation (17) can be combined with equations (13) and (15) to give

$$\alpha F^2 \geq \frac{2^5}{3^{5/2}} \left(\frac{c_{eu}^2 k'_e}{m} \right)^{3/2} \quad (18)$$

It can be seen that the stronger non-linearity and higher level of excitation amplitude are beneficial for meeting the requirement determined by equation (18) for an inflexion to occur. However, this will decrease the tuning range of the jump-up frequency.

Another condition is that the jump-down frequency should be kept higher than the excitation frequency. The jump-down frequency can be found by equating the two values in equation (10) to yield

$$1 - 4\zeta^2 U^2 - 3\beta\zeta^2 U^4 = 0 \quad (19)$$

and rearranging the expression gives

$$U_d \approx \sqrt{\frac{2}{3\beta} \left(\sqrt{1 + \frac{3\beta}{4\zeta^2}} - 1 \right)} \quad (20)$$

Substituting equation (20) into equation (10) yields the jump-down frequency of the frequency–amplitude curve as

$$\Omega_d \approx \sqrt{\frac{1}{2} \left(\sqrt{1 + \frac{3\beta}{4\zeta^2}} + 1 \right)} \quad (21)$$

As shown in Figure 3, a maximum equivalent damping exists when the damping c_2 is large enough. Substituting equations (6) and (7) into equation (21) leads to the corresponding damping c_2 versus the minimum jump-down frequency being obtained from $\frac{d\Omega_d}{dc_2} = 0$, which leads to the following expression

$$c_{2d} = \frac{k_1 + k_2}{\omega} \times \sqrt{\frac{k_2 \left(\sqrt{9k_1^2 + 4k_1 k_2 + 4k_2^2} - 3k_1 \right)}{2k_1 k_2 - 3k_1 \sqrt{9k_1^2 + 4k_1 k_2 + 4k_2^2} + 9k_1^2 + 2k_2^2}} \quad (22)$$

The corresponding equivalent stiffness coefficient k_{ed} and damping coefficient c_{2d} can then be obtained by substituting equation (22) into equations (6) and (7), respectively. Thus, the condition for keeping the oscillating point on the high-energy point can be expressed as

$$\Omega_{d \min} \geq \Omega \quad (23)$$

Using the same values of k_1 and αF^2 as previously obtained, and setting the mass at $m = 1$ kg, Figure 6 shows the minimum jump-down frequency $\Omega_{d \min}$ as a function of the stiffness coefficient ratio k_2/k_1 and αF^2 . It is obvious that the higher values of k_2/k_1 and αF^2 can increase the available minimum jump-down frequency of the system, which also indicates that the jump-down frequency can also be increased by employing a greater non-linearity in the stiffness and excitation amplitude. However, as discussed above, this will decrease the tunable jump-up frequency range. Therefore, the parameters k_2/k_1 and αF^2 should be appropriately selected.

Numerical examples

The parameters in Table 1 are used for simulation but under different excitation level F and stiffness

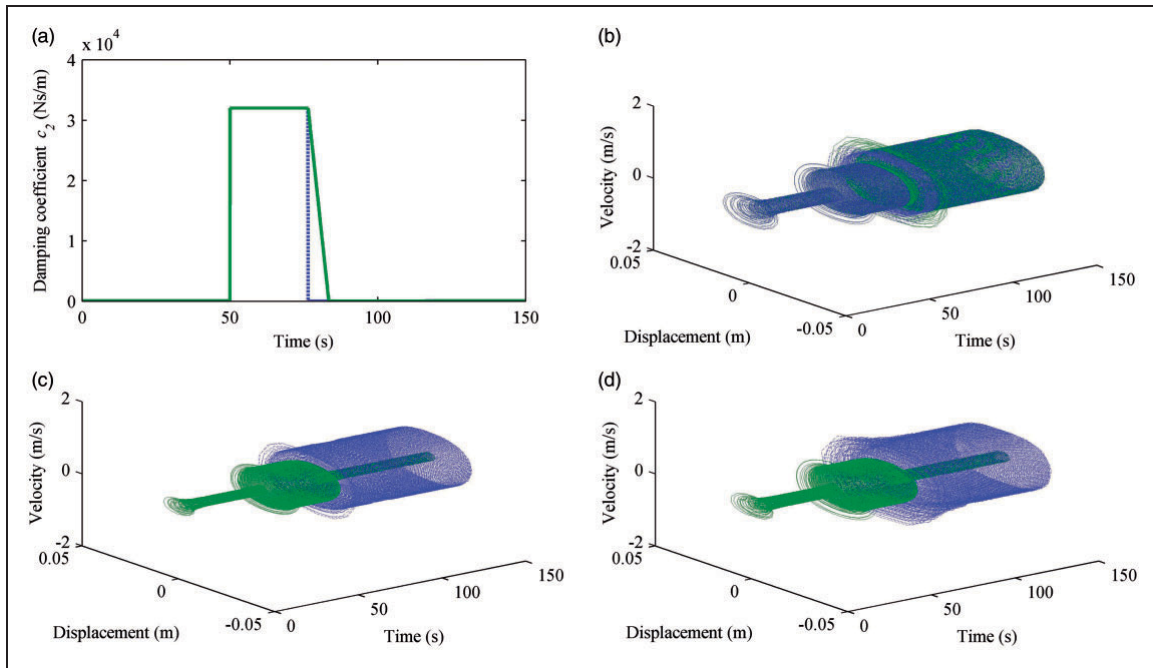


Figure 7. Variation of the damping coefficient and velocity vs displacement phase trajectories of the magnetic end mass (blue line: damping coefficient instantaneously tuned, and green line: damping coefficient slowly tuned): (a) changing the damping coefficient c_2 , (b) response with F and k_2 set to 3N and 1000 N/m, respectively, (c) response with F and k_2 set to 2N and 1000 N/m, respectively, and (d) response with F and k_2 set to 3N and 500 N/m, respectively.

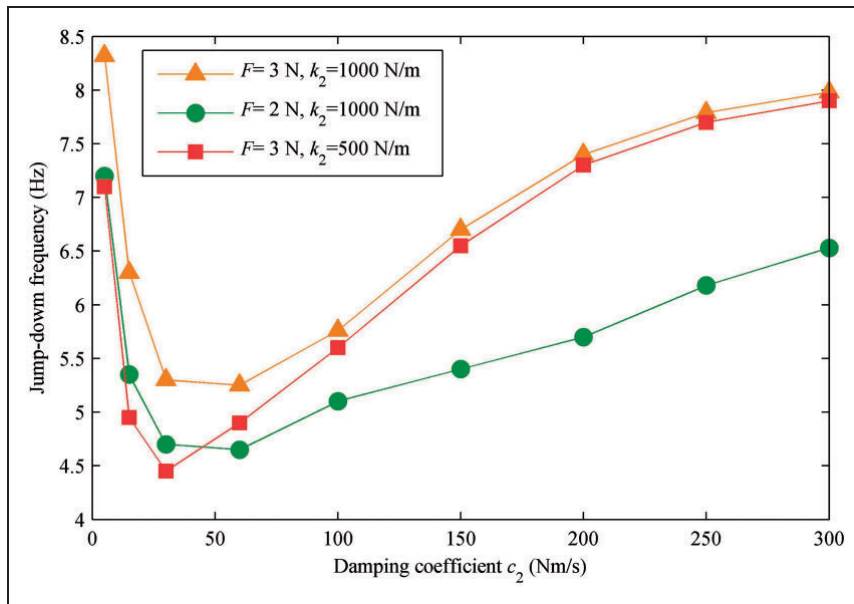


Figure 8. Jump-down frequency as a function of damping coefficient c_2 under various excitation levels and stiffness coefficients k_2 .

coefficient k_2 . Figure 7 presents the tuning process for the damping coefficient c_2 , and the corresponding velocity versus displacement phase trajectories of the magnetic end mass. As shown in Figure 7(b), the oscillating point jumps to the high-energy orbit with the increase in the damping coefficient, and then moves

further towards the maximum response point by decreasing c_2 and by setting F and k_2 equal to 3N and 1000 N/m, respectively.

However, when the excitation amplitude F is set to 2N, the condition defined by equation (23) cannot be satisfied, as shown in Figure 8, the minimum

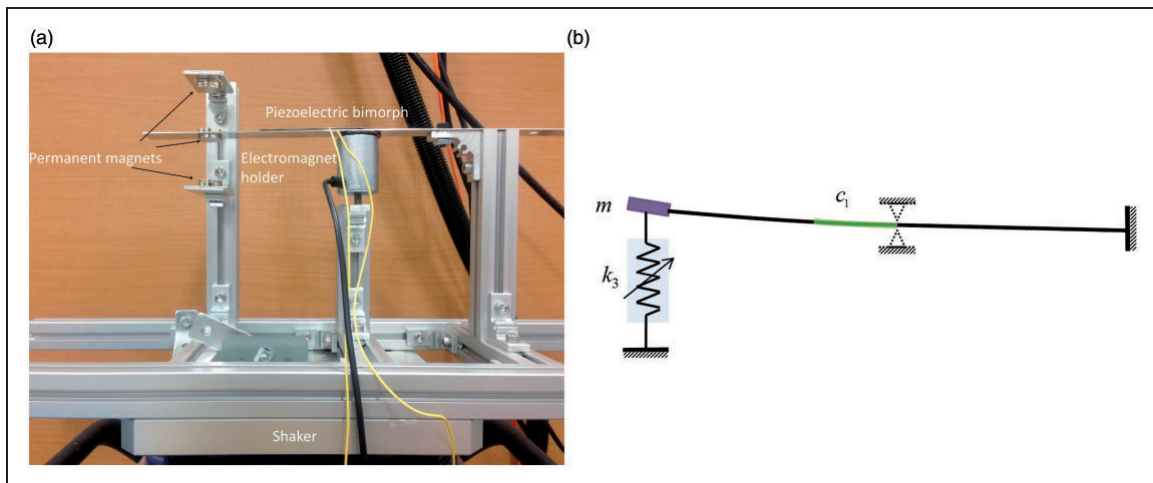


Figure 9. Experimentation setup: (a) photo of the experimental device and (b) the corresponding schematic diagram.

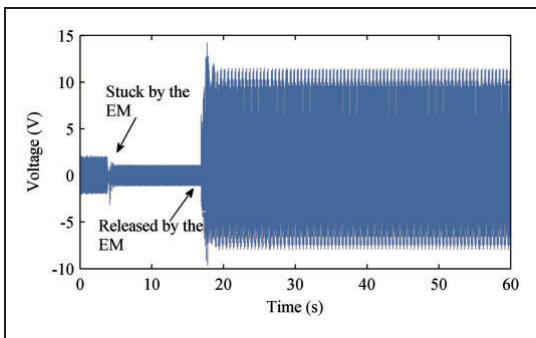


Figure 10. Measured output voltage on the load resistance.

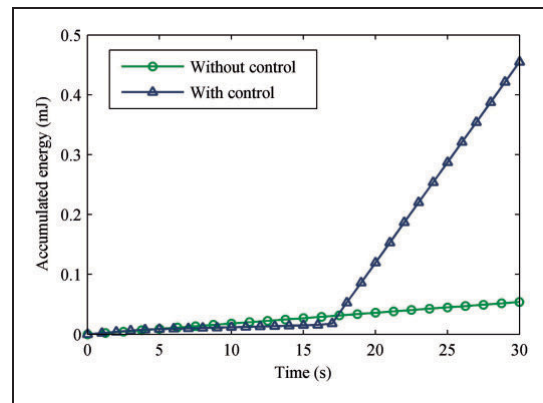


Figure 11. Cumulative energy on the load resistance.

jump-down frequency is smaller than the excitation frequency of 5.2 Hz. The oscillating point jumps to the low-energy orbit again during a decrease in the damping coefficient, which is shown in Figure 7(c) (green line). A similar response can be seen in Figure 7(d) (green line) when the stiffness coefficient k_2 is set to 500 N/m. The corresponding jump-down frequency as a function of the damping coefficient c_2 is also presented in Figure 8. It establishes that the smaller value of k_2/k_1 can decrease the available minimum jump-down frequency of the system in the process of damping variation.

The condition defined by equation (23) provides a limitation on the tuning procedure. However, from Figure 7(c) and (d) (blue line), it is interesting to find that another approach to triggering a jump to the high-energy orbit is by instantaneously decreasing the damping coefficient c_2 , when the condition defined by equation (23) is not satisfied. It is known that the steady-state orbit is also significantly dependent upon the initial conditions. This is evaluated by using the basin of attraction obtained by choosing the initial conditions from the lattice points in the phase plane and then solving the equation of motion numerically until the trajectory converges to one of the steady-state

solutions.¹⁹ As mentioned previously, by increasing the controllable damping c_2 , the operating point can jump to the high-energy orbit (see point B in Figure 4). Then, when c_2 instantaneously decreases to the initial value this could be regarded as an initial condition to be applied to the oscillator, and this initial condition is caused by the response of the oscillator at point B in Figure 4. If the initial conditions can lead to the basin of attraction for the high-energy solution then the oscillator will stabilise on the corresponding high-energy orbit. This approach gives a possible solution to the limitation problem defined by equation (23).

Experimental tests

This section describes the experimental tests performed to validate the proposed method. A picture of the fabricated energy harvester attached to the shaker table (m060, IMV Corp., Japan) is shown in Figure 9, in which three permanent magnets are arranged in a repulsive configuration to provide the cubic non-linear stiffness,¹⁷ and where the magnetic end mass attached to the piezoelectric beam is aligned

with respect to the symmetrically fixed permanent magnets (top and bottom magnets) in the vertical direction. The top and bottom magnets are symmetrically attached to sliders on a rail and this configuration allows the distance to be adjusted equally on each side, and so the natural frequency of the device is set to 16.3 Hz. It should be mentioned that an electrical damper is favourable for the experiment and that it can be fabricated using a linear DC motor or a DC generator coupled with a ball screw so that it can produce a high level of damping. The damping could be tuned using a variable resistance,²⁵ with the advantage that electrical energy can be harvested by the controllable damper, even during the tuning process. However, because of the mass of the linear DC motor and the equivalent mass of the moment of inertia of the ball screw and rotor, it becomes rather difficult to achieve a very high damping ratio, as expected in an ideal experimental device. As an alternative, a small piece of ferrous metal is attached to the beam and an electromagnetic restraining device is placed under it with a small gap between them. And the gap is set small enough to minimise the influence on the response caused by the initial displacement when the beam is released. The piezoelectric beam can be regarded as two springs connected at the location of the small piece of ferrous metal. The electromagnetic restraining device is used to simulate the conditions that $c_2 \rightarrow 0$ and $c_2 \rightarrow \infty$ by restraining and releasing the beam, respectively. On the other hand, the piezoelectric bimorph provides the electrical damper c_1 for energy harvesting. A schematic diagram of the ideal energy harvester is also presented on the right-hand side of Figure 9.

Figure 10 presents the measured voltage on a load resistance of 1 M when the energy harvester is subjected to a base excitation of 0.62 m/s^2 at 18 Hz. It can be seen that the output voltage decreases when the beam is held by the electromagnet restraining device, because the oscillating point moves to the lower frequency side of the frequency–response curve, and the natural frequency of the system is measured to be 23.25 Hz. When the beam is released by the electromagnet it can be seen that it jumps to the oscillating point which is close to the jump-down point on the high-energy orbit, and this validates the proposed solution to the limitation defined by equation (23). Figure 11 compares the cumulative generated energy when the harvester is operated on the low-energy orbit and the condition with damping variation.

Conclusions

This study has investigated the principle of stabilising the high-energy response of a non-linear vibrational energy harvester that is stiffness tunable, by changing the damping coefficient of the system. The mathematical model of the energy harvester with equivalent stiffness and damping coefficients is

derived, and their influence on the frequency–response curve during the tuning process is also presented. The ratio between the stiffness coefficients of the two springs connected in series, the non-linear stiffness, and the excitation amplitude all apparently affect the available tuning range of the system, especially the minimum jump-down frequency when decreasing the controllable damping coefficient, and this provides a limitation. However, through numerical study and experimentation it was established that instantaneous variation of the damping was a possible approach to the solution. The method proposed in this paper can trigger a jump from the low-energy orbit to the high-energy orbit, thus enhancing the availability of harvestable energy from external harmonic vibration. Compared with the approach of self-excitation for stabilising the high-energy orbit by consuming part of the harvested electrical energy, and mechanical methods for stiffness tuning,^{19–21} the proposed method requires little additional energy consumption, as demonstrated in this study. Certainly, a circuit is needed to vary the damping and this is inevitable for any active tuning method. However, this proposed method is a potentially easy way of implementation and can be considered to be a promising approach to promoting the practical implementation of a hardening monostable energy harvester.

Conflict of interest

None declared.

Funding

The study was supported by the Institute of Industrial Science at the University of Tokyo, Japan. The first author also wishes to record his sincere gratitude to the China Scholarship Council for the financial support (Grant no: 201206050004).

References

1. Foisal AMd, Hong C and Chung G. A resonant frequency self-tunable rotation energy harvester based on magnetoelectric transducer. *Sens Actuat A: Phys* 2013; 194: 6–24.
2. Torah R, Glynn-Jones P, Tudor M, et al. Self-powered autonomous wireless sensor node using vibration energy harvesting. *Meas Sci Technol* 2008; 19: 125202.
3. Tang L, Yang Y and Soh CK. Toward broadband vibration-based energy harvesting. *J Intel Mater Syst Struct* 2010; 21: 1869–1897.
4. Leland ES and Wright PK. Resonance tuning of piezoelectric vibration energy scavenging generators using compressive axial preload. *Smart Mater Struct* 2006; 15: 1413–1420.
5. Challa VR, Prasad MG, Shi Y, et al. A vibration energy harvesting device with bidirectional resonance frequency tunability. *Smart Mater Struct* 2008; 17: 015035.
6. Kulah H and Najafi K. Energy scavenging from low-frequency vibrations by using frequency up-conversion for wireless sensor applications. *IEEE Sens J* 2008; 8: 261–268.

7. Eichhorn C, Goldschmidtboeing F and Woias P. A frequency tunable piezoelectric energy converter based on a cantilever beam. In: *Proceedings of power MEMS*, Sendai, Japan, 2008, pp.309–312.
8. Shahruz SM. Design of mechanical band-pass filters for energy scavenging. *J Sound Vib* 2006; 292: 987–998.
9. Shahruz SM. Limits of performance of mechanical band-pass filters used in energy scavenging. *J Sound Vib* 2006; 292: 449–461.
10. Rastegar J and Murray R. Novel two-stage piezo-electric-based electrical energy generators for low and variable, speed rotary machinery. *Proc SPIE* 2010; 7288: 72880B.
11. Li M, Wen Y, Li P, et al. A resonant frequency self-tunable rotation energy harvester based on magneto-electric transducer. *Sens Actuat A: Phys* 2013; 194: 16–24.
12. Ayala-Garcia IN, Mitcheson PD, Yeatman EM, et al. Magnetic tuning of a kinetic energy harvester using variable reluctance. *Sens Actuat A: Phys* 2013; 189: 266–275.
13. Green PL, Worden K, Atallah K, et al. The benefits of Duffing-type nonlinearities and electrical optimisation of a mono-stable energy harvester under white Gaussian excitations. *J Sound Vib* 2012; 331: 4504–4517.
14. Mann BP, Gorman DG and Owens BA. Investigations of a nonlinear energy harvester with a bistable potential well. *J Sound Vib* 2010; 329: 1215–1226.
15. Stanton SC, McGehee CC and Mann BP. Nonlinear dynamics for broadband energy harvesting: investigation of a bistable piezoelectric inertial generator. *Physica D* 2010; 239: 640–653.
16. Zheng R, Nakano K, Hu H, et al. An application of stochastic resonance for energy harvesting in a bistable vibrating system. *J Sound Vib* 2014; 333: 2568–2587.
17. Mann BP and Sims ND. Energy harvesting from the nonlinear oscillations of magnetic levitation. *J Sound Vib* 2009; 319: 515–530.
18. Stanton SC, McGehee CC and Mann BP. Reversible hysteresis for broadband magneto-piezo-elastic energy. *Appl Phys Lett* 2009; 95: 174103.
19. Masuda A, Senda A, Sanada T, et al. Global stabilization of high-energy response for a Duffing-type wide-band nonlinear energy harvester via self-excitation and entrainment. *J Intell Mater Syst Struct* 2013; 24: 1598–1612.
20. Zhu D, Roberts S, Tudor J, et al. Closed loop frequency tuning of a vibration-based microgenerator. In: *Proceedings of power MEMS*, Sendai, Japan, 2008, pp.229–232.
21. Su D, Nakano K, Zheng R, et al. Investigations of a stiffness tunable nonlinear vibrational energy harvester. *Int J Struct Stab Dyn* 2014; 14: 1440023.
22. Liu Y, Matsuhisa H and Utsuno H. Semi-active vibration isolation system with variable stiffness and damping control. *J Sound Vib* 2008; 313: 16–28.
23. Johnson DR, Harne RL and Wang KW. A disturbance cancellation perspective on vibration control using a bistable snap-through attachment. *J Vib Acoust* 2014; 136: 031006.
24. Brennan MJ, Kovacic I, Carrella A, et al. On the jump-up and jump-down frequencies of the Duffing oscillator. *J Sound Vib* 2008; 318: 1250–1261.
25. Nakano K and Suda Y. Combined Type self-powered active vibration control of truck cabins. *Vehicle Syst Dyn* 2004; 41: 449–473.